

CFD Based Comparative Analysis of Different Ribs with Varying and Same Height in Rectangular Duct

Mr. Sandeep Kumar Karole
PG Student
Department of Mechanical Engineering
Scope Collage of Engineering, Bhopal (M.P.)

Mr. Ishwar Singh
Professor
Department of Mechanical Engineering
Scope Collage of Engineering, Bhopal (M.P.)

Abstract

A computational study are conducted to assess turbulent forced convection heat transfer and friction loss behaviors for air flow through a constant heat flux channel fitted with House shaped ribs at same height and uniformly varying height shaped ribs. Ten rib arrangements, namely, in-line and staggered arrays, are introduced. Measurements are carried out for a rectangular channel of aspect ratio, $AR=1$ and height, $H=1.598$ mm with single rib height, $e=1.598$ mm and rib pitch, $P=22.91$ mm, Uniformly Varying Height up to 2 mm. The flow rate is in terms of Reynolds numbers based on the inlet hydraulic diameter of the channel in a range of 4000 to 12,000. The computational results show a significant effect of the presence of the ribs on the heat transfer rate and friction loss over the smooth wall channel. The in-line rib arrangement provides higher heat transfer and friction loss than the staggered one for a similar mass flow rate. In comparison, the isosceles triangular, house-shaped, right-angle triangular, reverse pentagonal. Pointing downstream yields the highest increase in both the Nusselt number and the pressure drop but the reverse pentagonal (UVH) ribs and right angle triangular (UVH) with staggered array shows better thermal performance over the others.

Keywords: Computational analysis, Friction factor, Heat Transfer, Pressure Drop, ribbed channel

I. INTRODUCTION

In the cooling channel or channel heat exchanger design, rib, fin or baffle turbulators are often employed in order to increase the convective heat transfer rate leading to the compact heat exchanger and increasing the efficiency. For decades, rib turbulators have been applied in high-performance thermal systems due to their high thermal loads. The cooling or heating air is supplied into the passages or channels with several ribs to increase the stronger degree of cooling or heating levels over the smooth wall channel. The use of rib turbulators completely results in the change of the flow field and hence the variation of the local convective heat transfer coefficient. The presence of a transverse rib assists to induce the main stream separation first, and to generate a recirculation zone ahead of it and then reattachment over the rib itself. A further separation occurring after the rib and creating a second recirculation zone behind the rib is followed by another reattachment at the channel wall. If several ribs exist and their pitch is sufficiently larger than the rib height, these flow patterns will reoccur along the channel wall. The use of ribs increases not only the heat transfer rate both for the increased turbulence degree and for the effects caused by reattachment but also substantial the pressure loss. The rib geometry and arrangement in the channel also alter the flow field resulting in different convective heat transfer distribution. In particular, the angled ribs, the rib cross section, the rib-to-channel height ratio and the rib pitch-to-height ratio are all parameters that influence both the convective heat transfer coefficient and the overall thermal performance.

J.C. Han, J.S. Park, M.Y. Ibrahim. [1]- Fig. 5.1 shows the geometry of the cooling channel analyzed in this study; the channel was roughened by square ribs. The channel aspect ratio ($AR = W/H$) was 2.0, and the hydraulic diameter (D_h) was 34 mm. In total, 10 ribs were placed on one wall in the computational domain. The pitch-to-hydraulic diameter ratio (p/D_h) was 10.0 and the rib height-to-hydraulic diameter (h/D_h) was 0.047, which are the same as that used by Han et al.

C.G. Spezial, S. Sarkar, T.B. Gatski [2]- Turbulence was analyzed using the Reynolds stress model with the Speziale-Sarkar-Gatski (SSG) pressure-strain model. The SSG model for the pressure-strain correlation terms in the transport equations for the Reynolds stress components was developed by considering the invariance with dynamical systems theory. The SSG Reynolds stress model was expected to provide accurate predictions especially for flows with a strong streamline curvature.

M.E. Taslim, S.D. Spring [3]-Previous works- showed that, when the rib cross section is changed from a square to a rectangle (i.e., the rib width to- height ratio (e/h) increases or decreases from unity), the area averaged Nusselt number decreases at Reynolds numbers of 5000–50,000. The heat transfer coefficient for the isosceles triangular rib (Case 2) is known to increase as the rib width-to-rib height ratio is increased from 1.0 to 2.0 at Reynolds numbers of 20,000–60,000.

M.E. Taslim, S.D. Spring [4]- showed that the heat transfer enhancements with these triangular ribs were higher than those with the rectangular ribs for the entire range of tested rib width-to-height ratios at Reynolds numbers of 4000–16,000.

C.O. Olsson, B. Sunden[5] tested two ribbed radiator tubes with airflow. The air heat transfer data were taken with constant wall temperature and the data provide the axially averaged heat transfer coefficient over the tube length. The enhanced tubes showed higher friction factors than the smooth tube in both laminar and turbulent regions. However, as the Reynolds number decreased in the strictly laminar region, the friction factors tended to converge and approach the smooth tube value. Also, the laminar-turbulent transition Reynolds number decreased as the friction factor increased. Similar to the friction behavior, the Colburn j factors also tended to converge at low Reynolds numbers, and approached the smooth tube value. However, in contrast to the friction factors, the j factors did not show a clear laminar-turbulent transition.

J. C. Han, L. R. Glicksman and W. M. Rohsenow[6]- Based on the law of the wall similarity and the application of a heat-momentum transfer analogy. General friction and heat-transfer correlations have been obtained by taking into account the effect of geometrically non-similar parameters. Friction and heat-transfer correlations agree well with other investigators. Although discrepancies are evident when the correlations are compared to data reduced by use of the Hall type transformation.

Akira Murata, Sadanari Mochizuki[7]- Effect of rib orientation and channel rotation on heat transfer in a two-pass square channel with 1800 sharp turns was numerically investigated by using the large eddy simulation with a Lagrangian dynamic sub grid-scale model. In the stationary condition, the heat transfer in and after the turn was increased, and it was dominated by the sharp-turn induced flow field. In the rotating condition, the highest rotating speed caused deteriorated heat transfer on the pressure surface of the straight pass. When the channel was rotated, the flow and heat transfer in the turn was mainly dominated by the sharp turn and the Coriolis force effects. For the highest rotation number case of this study ($Ro = 2$), the Nusselt number on the pressure surface of the straight pass was deteriorated due to the suppressed turbulence, and an interesting alternating flow behavior was observed.

M. Amro, B. Weigand, R. Poser, M. Schnieder [8]- The present study investigates the internal cooling in a triangular channel with a rounded edge as a model of a leading edge cooling channel for a gas turbine blade. A transient liquid crystal method is used to measure the heat transfer. Experimental results are reported for a number of new 3D rib configurations for Reynolds numbers between 50 000 and 200 000. From the experimental results it has been found that 600. ribs provide in general higher heat transfer enhancements than 45 deg. ribs. However, this results in extremely high friction factors for the 600. ribs.

S.W. Chang, T.-M. Liou, K.F. Chiang, G.F. Hong [9]- A novel heat transfer enhancement (HTE) roughness with V-shaped ribs and deepened scales is devised. Performances of heat transfer and pressure drop in a rectangular channel fitted with such HTE surfaces are experimentally examined for both forward and backward flows in the Re range of 1000–30000. Relative to the smooth-walled pipe flow conditions, HTE ratios for the present test channel with forward and backward flows, respectively, reach 9.5–13.6 and 9–12.3 for laminar flows and 6.8–6.3 and 5.7–4.3 for turbulent flows. Comparisons of heat transfer data, pressure-drop measurements and thermal performance factors with previous results collected from varieties of HTE devices demonstrate the superiorities of this compound HTE device.

Pongjet Promvongse, Chinaruk Thianpong[10]- The rib cross-sections used in the present study are triangular (isosceles), wedge (right-triangular) and rectangular shapes. Two rib arrangements, namely, in-line and staggered arrays, are introduced. Measurements are carried out for a rectangular channel of aspect ratio, $AR=15$ and height, $H=20$ mm with single rib height, $e=6$ mm and rib pitch, $P=40$ mm. The flow rate is in terms of Reynolds numbers based on the inlet hydraulic diameter of the channel in a range of 4000 to 16,000. In comparison, the wedge rib pointing downstream yields the highest increase in both the Nusselt number and the friction factor but the triangular rib with staggered array shows better thermal performance over the others. The use of the rib turbulators with $e/H=0.3$ causes a very high-pressure drop increase, specially for the in-line rib arrangement and also provides considerable heat transfer augmentations, $Nua/Nu_0=2.6-4.4$, depending on rib geometry. Nusselt number augmentation tends to increase with the rise of Reynolds number.

Arvind Kumar, J.L. Bhagoria, R.M. Sarviya[11]- In solar air heater by using discrete W-shaped roughness on one broad wall of solar air heater with an aspect ratio of 8:1, the roughened wall being heated while the remaining three walls are insulated. The experiment encompassed Reynolds number (Re) range from 3000 to 15,000, relative roughness height (e/D_h) in the range of 0.0168–0.0338, relative roughness pitch (p/e) 10 and the angle of attack (α) in the range of 30–75°. The effect of parameters on the heat transfer and friction are compared with the result of smooth duct under similar flow conditions. The comparison of experimental values of Nusselt number and friction factor and those predicted by the correlation shows that all 140 data points lie within the deviation range of $\pm 10\%$. Liu [14]- performed computational simulations to investigate the heat transfer performances of rectangular ($e/h = 2.0$), isosceles triangular (Case 2, $e/h = 1.0$), isosceles trapezoidal (Case 15, $e/h = 2.0$), and semicircular (Case 16, $e/h = 1.0$) ribs for Reynolds numbers of 5000–10,000. The isosceles triangular rib showed the best heat transfer performance followed by the isosceles trapezoidal rib, rectangular rib, and semicircular rib in order.

Wongcharee [15]- numerically investigated the effect of the rib shape on the heat transfer and pressure drop characteristics of a rectangular channel. They tested seven types of rib shapes: rectangular, triangular, cylindrical, concave–concave, convex–concave, long concave–short concave, and long convex–short concave. They reported that the triangular rib showed the highest heat transfer. The modified ribs with a concave front surface (i.e., the concave–concave and long concave–short concave ribs) gave higher heat transfer rates than the modified ribs with a convex front surface (i.e., convex–concave and long convex–short concave ribs) when the Reynolds number was 3000–7000.

Manca[16]- numerically investigated the thermal performance of various rib shapes (rectangular, square, triangular, rectangular-trapezoidal, and isosceles-trapezoidal) in the cooling channel. The triangular ribs gave the best heat transfer rate among these rib shapes.

Giovanni Tanda [17]- An experimental investigation of forced convection heat transfer in a rectangular channel (aspect ratio $AR = 5$) with angled rib turbulators, inclined at 45° , is presented. The angled ribs were deployed with parallel orientations on one or two surfaces of the channel. The convective fluid was air, and the Reynolds number varied from 9000 to 35,500.

Mi-Ae Moon, Min-Jung Park, Kwang-Yong Kim[24]- The heat transfer and friction loss performances of rib-roughened rectangular cooling channels having a variety of cross-sectional rib shapes were analyzed using three-dimensional Reynolds-averaged Navier– Stokes equations. Numerical simulations were conducted for sixteen rib shapes: square, isosceles triangular, fan-shaped, house-shaped, reverse cut-trapezoidal, cut-trapezoidal, reverse boot-shaped, boot-shaped, reverse right-angle triangular, right-angle triangular, reverse pentagonal, pentagonal, reverse right-angle trapezoidal, right-angle trapezoidal, isosceles trapezoidal, and semicircular ribs. The ratios of pitch, height, and width of the rib to hydraulic diameter of the channel were set to 10, 0.047, and 0.047, respectively.

II. CROSS-SECTIONAL RIB SHAPES

Fig.1.1 shows the various ribs with different cross-sectional shapes tested in this work; these were installed in the rectangular channel shown in Fig.1.2. Four ribs were tested: isosceles triangular, house-shaped, right-angle triangular, reverse pentagonal. These were arranged in a regular sequence, as shown in Fig.1.2. These rib shapes were characterized inside a square, as shown in Fig.1.1. The ratios of the rib width-to-hydraulic diameter of the channel and rib width-to-rib height were kept constant at 0.0467 and 1.0, respectively. The following rib shapes have already been investigated by many researchers for heat transfer enhancement: square (Case1), isosceles triangular(Case2), fan-shaped(Case3), house-shaped(Case4), reverse cut-trapezoidal(Case5), cut-trapezoidal(Case6), reverse boot-shaped(Case7), boot-shaped(Case8), reverse right-angle triangular(Case9), right-angle triangular(Case10), reverse pentagonal(Case11), pentagonal(Case12), reverse right-angle trapezoidal(Case13), right-angle trapezoidal(Case14), isosceles trapezoidal(Case15), and semicircular(Case16) ribs.

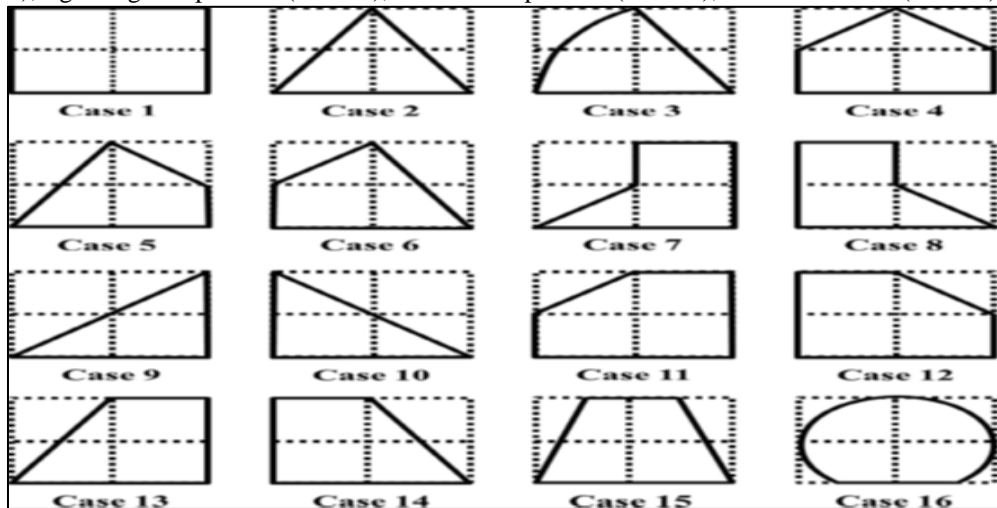


Fig. 1: Cross-Sectional RIB Shapes

III. MODAL AND ANALYSIS

In this chapter I have study in the rectangular duct with ribs arrange at same height (SH) and uniformly varying height (UVH). In this study the thermal properties, Reynolds number are same at all condition and all case. I have CFD analysis at different cases: isosceles triangular, house-shaped, right-angle triangular, reverse pentagonal.

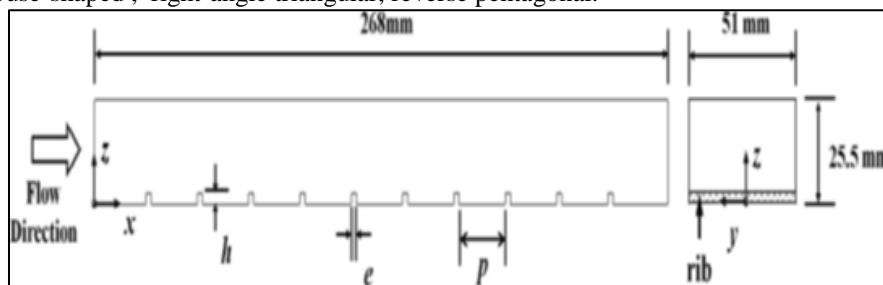


Fig. 2: Geometric parameters and computational domain.

Then the solutions for density and Temperature are used for finding the pressure using the equation of state. When fluid is incompressible the density is not linked to pressure, a guess-and-check technique such as SIMPLE is required in order to solve

the entire flow field. The working fluid in all cases is air. The properties of the working fluid (air) and top plate material (aluminum) have been assumed to remain constant at average bulk temperature. The thermo-physical properties of working fluid and top plate are illustrated in Table.

Table -1.1:
Properties of the working fluid (air) and Rectangular duct

Properties	Working fluid (air)	Top plate(aluminum)
Density (kgm^{-3})	1.225	2719
Specific heat c_p	1006.43	871
Viscosity (Nsm^{-2})	1.7894×10^{-5}	--
Thermal conductivity k ($Wm^{-1}k^{-1}$)	0.0242	202.4

After defining the computational domain, non-uniform mesh is generated. In creating this mesh, it is desirable to have more cells near the plate because we want to resolve the turbulent boundary layer, which is very thin compared to the height of the flow field. After generating mesh, boundary conditions have been specified. We will first specify that the left edge is the duct inlet and right edge is the duct outlet. Top edge is top surface and bottom edges are inlet length, outlet length. All internal edges of rectangle 3D duct are defined as turbulator wall. Meshing of the domain is done using ANSYS 14.5 software.

Generation of 3D CAD model of Rectangular Duct using Unigraphics. Then import the CAD model into Ansys Design modeler in parasolid format (.x_tl or .x_t).

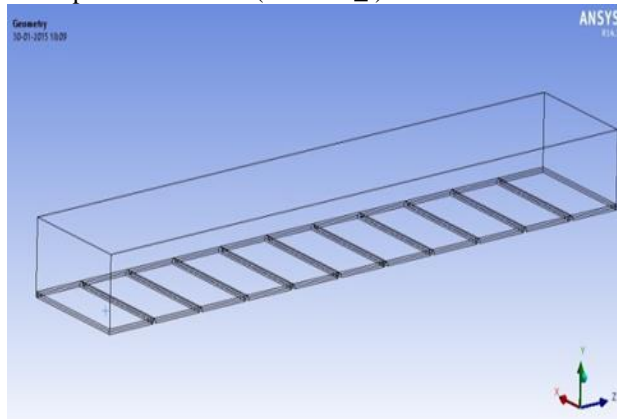


Fig. 2.1: CAD Model

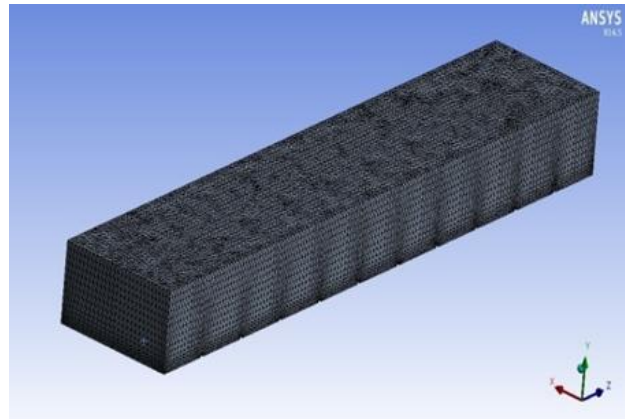


Fig. 2.2: Meshing

IV. NUMERICAL ANALYSIS

As the boundary condition for the computational domain shown in Fig. 2.2, a uniform velocity profile was adopted at the inlet with a Reynolds number of 30,000 based on the channel hydraulic diameter. The inlet temperature of the working fluid (air) was kept constant at 298.15 K, and a specific pressure was adopted at the outlet. A uniform heat flux (300 W/m²) was specified on the roughened wall, including the surface of the ribs. A no-slip condition was applied to all the surfaces. All the surfaces except the roughened surface were regarded as adiabatic. The turbulence level at the inlet was specified as 5.0%. A hexahedral grid system was used as shown in Fig. 2.2. The grids were concentrated at the wall region to resolve the high velocity gradient near the wall. The minimum grid spacing was maintained at 0.01 of the channel height, which corresponded to the wall coordinate y^+ of the order of 1.0. The root mean square (RMS) relative residual values of all flow parameters were set to 1.0×10^{-5} , and energy and mass imbalances of less than 0.003% were adopted as convergence criteria. The solver finished a single simulation in 4–5 h with approximately 1000 iterations using an Intel i7 2.4 GHz CPU.

V. PERFORMANCE PARAMETERS

In this study, the heat transfer and friction factor were used to define the performance parameters of an internal cooling channel with various rib shapes. The performance parameter related to heat transfer was defined according to the Nusselt number:

$$\text{Relative roughness height} = e/D \quad \dots \dots \dots (5.1)$$

$$\text{Hydraulic Diameter (D)} = 4WH/2(W+H) \quad \dots \dots \dots (5.2)$$

H=Height of the duct in m, W=Width of the duct in m

$$\text{Velocity of air (V)} = Re(v)/D \quad \dots \dots \dots (5.3)$$

v= Kinematic viscosity of air in m²/sec, V= Velocity of air

$$\text{Heat transfer Coefficient (h)} \quad Q=hA \Delta T \quad \dots \dots \dots (5.4)$$

Average heat transfer coefficient (h) can be obtained directly from FLUENT.

Nusselt Number for roughened duct $Nur=hD/K$ (5.6)

Where k is the thermal conductivity of air and D is the hydraulic diameter.

Nusselt Number for smooth duct $Nus=0.023Re^{0.8}Pr^{0.4}$ (5.7)

Nusselt Number for smooth roughened duct can be obtained by Dittus-Boelter correction.

Friction factor for roughened duct $f = \Delta p Dh / 2P\rho u_{in}^2$ (5.8)

Friction factor for smooth roughened duct can be obtained by Blasius correction. Average pressure drop (Δp) can be obtained directly from FLUENT.

A. Revers Pentagonal Shape- Case I & Case II:

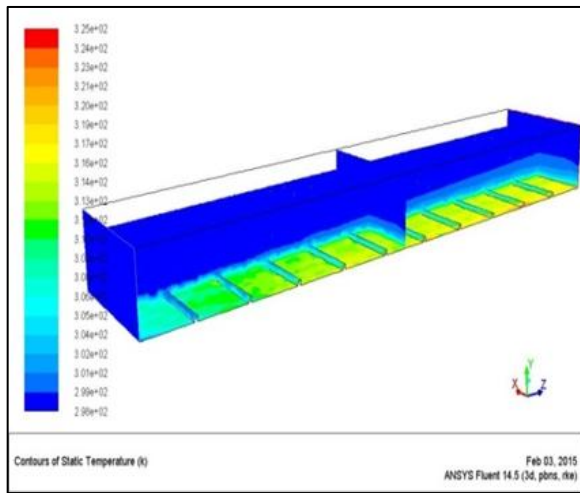


Fig. 3: Static Temperature at SH

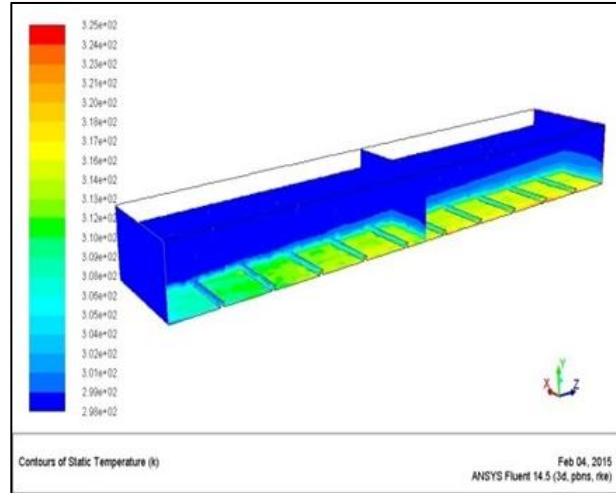


Fig. 4: Static Temperature at UVH

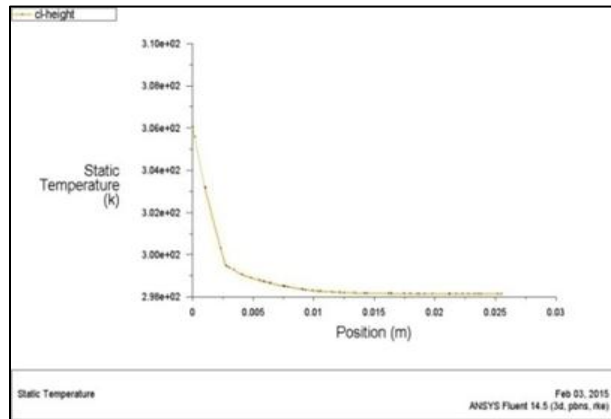


Fig. 5: Static Temperature with respect to height at SH

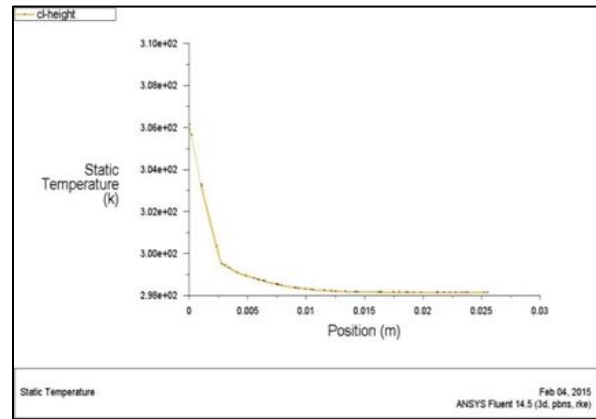


Fig. 6: Static Temperature with respect to height at UVH

B. Triangular Shape - Case III & Case IV:

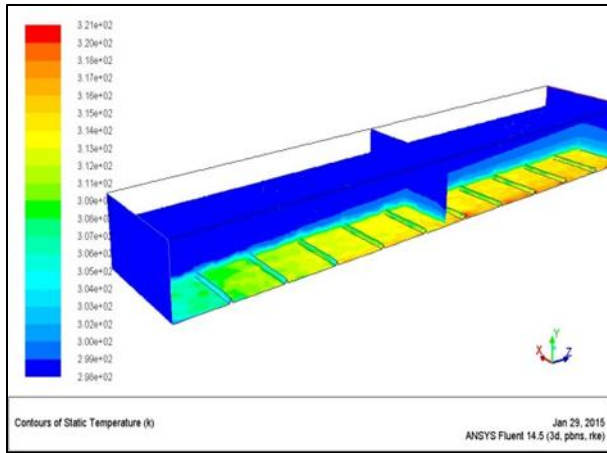


Fig. 7: Static Temperature at SH

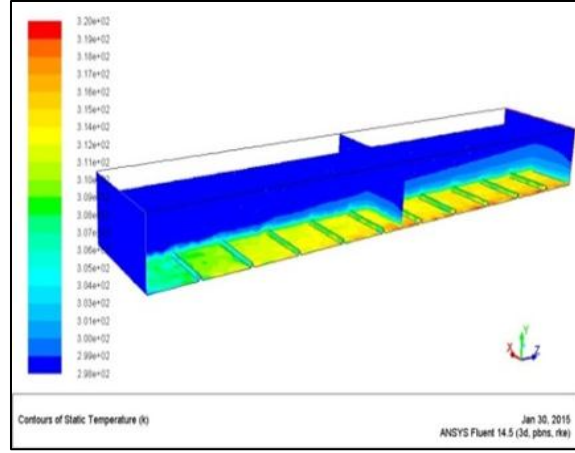


Fig. 8: Static Temperature at UVH

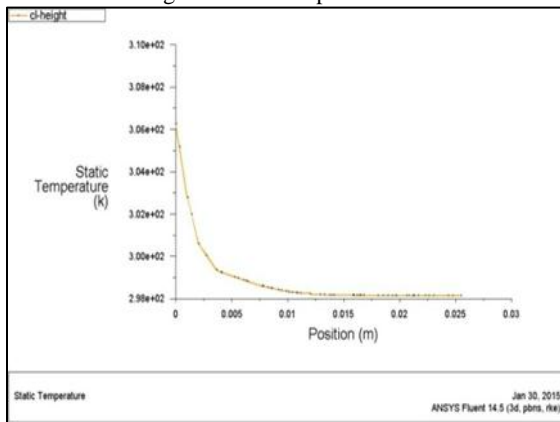


Fig. 9: Static Temperature with respect to height at SH

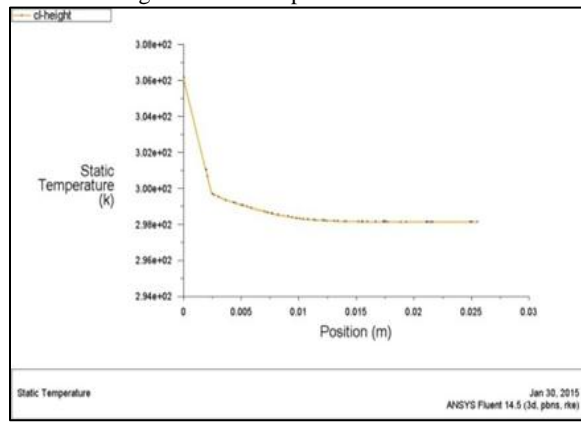


Fig. 10: Static Temperature with respect to height at UVH

C. House Shape- Case V & Case VI:

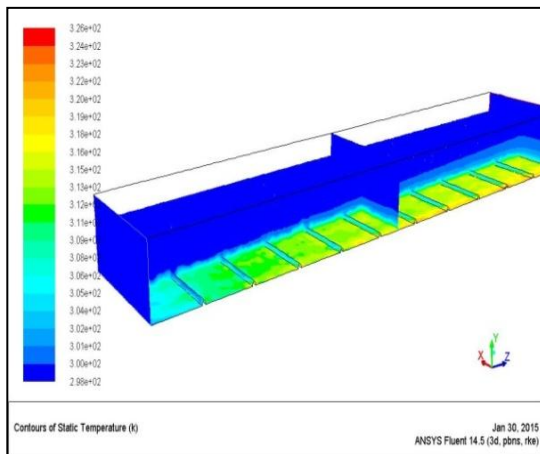


Fig. 11: Static Temperature at SH

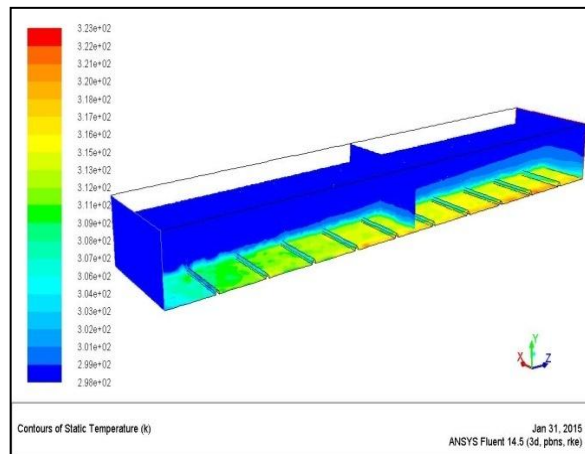


Fig. 12: Static Temperature at UVH

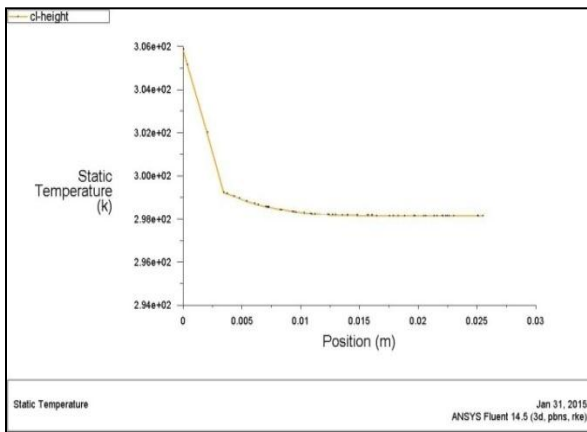


Fig. 13: Static Temperature with respect to height at SH

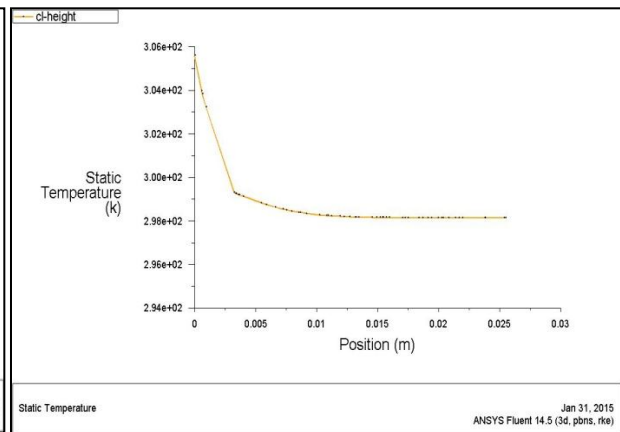


Fig. 14: Static Temperature with respect to height at UVH

D. Right Angle Triangular- Case VII & Case VIII:

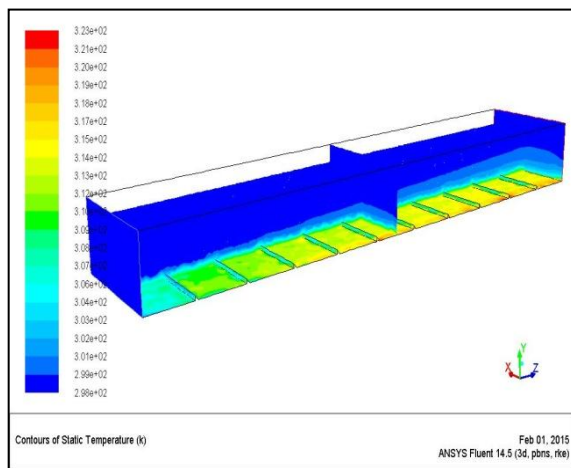


Fig. 15: Static Temperature at SH

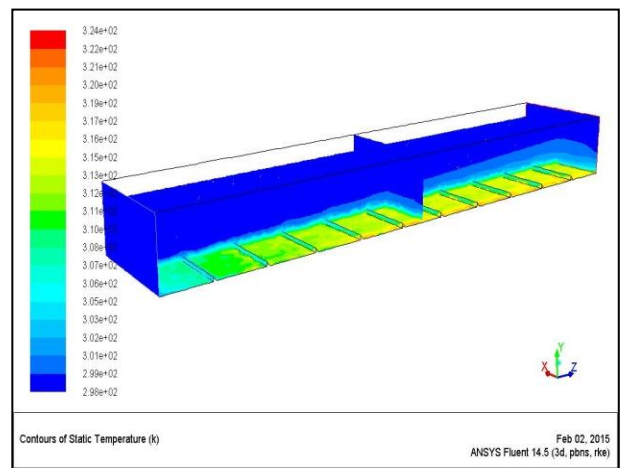


Fig. 16: Static Temperature at UVH

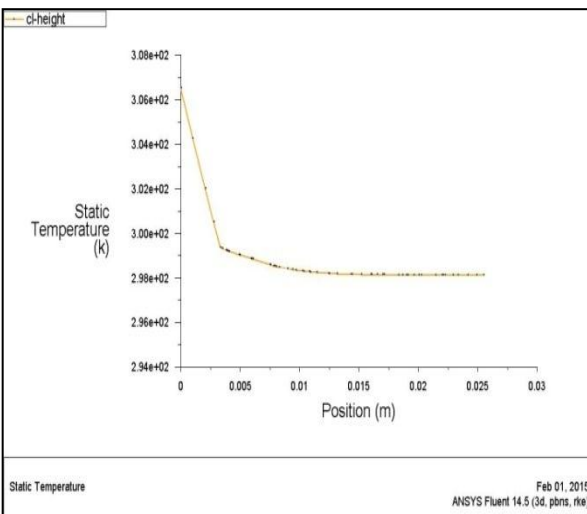


Fig. 17: Static Temperature with respect to height at SH

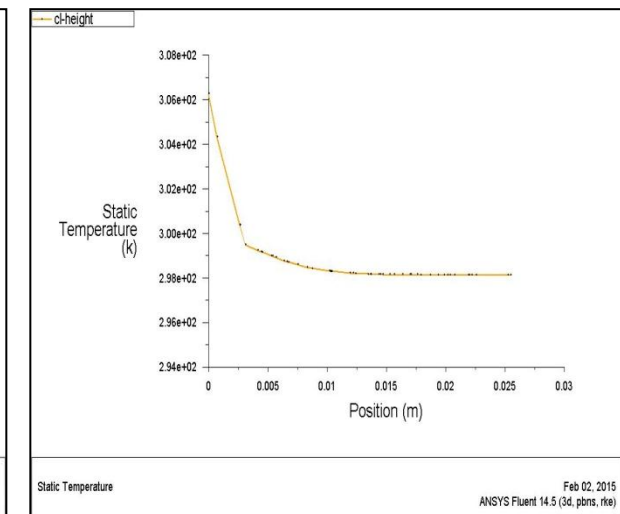


Fig. 18: Static Temperature with respect to height at UVH

VI. RESULTS AND DISCUSSION

In the present work, CFD Analysis measurements of both heat transfer and friction loss in channels with different rib shapes are presented. Measurements were conducted in a channel of aspect ratio, AR=1 for four rib arrangements at S.H and U.V.H with each rib shape, over a range of Reynolds numbers as mentioned earlier.

A. Verification Of Smooth Channel:

The present , CFD Analysis results on heat transfer and friction characteristics in a smooth wall channel are first validated in terms of Nusselt number and friction factor. The Nusselt number and friction factor obtained from the present smooth channel are, respectively, compared with the correlations of Dittus–Boelter and Blasius found in the open literature for turbulent flow in ducts. Correlation of Dittus–Boelter

$$Nu = 0.023Re^{0.8}Pr^{0.4}$$

for heating Correlation of Blasius(1)

$$f = 0.316Re^{-0.25}$$

for $3000 \leq Re \leq 20,000$(2)

Fig.19 shows, respectively, a comparison of Nusselt number and friction factor obtained from the present work with those from correlations of Eqs. (1) and (2). In the figures, the present results reasonably agree well within $\pm 10\%$ for both friction factor correlation of Blasius and Nusselt number correlation of Dittus–Boelter.

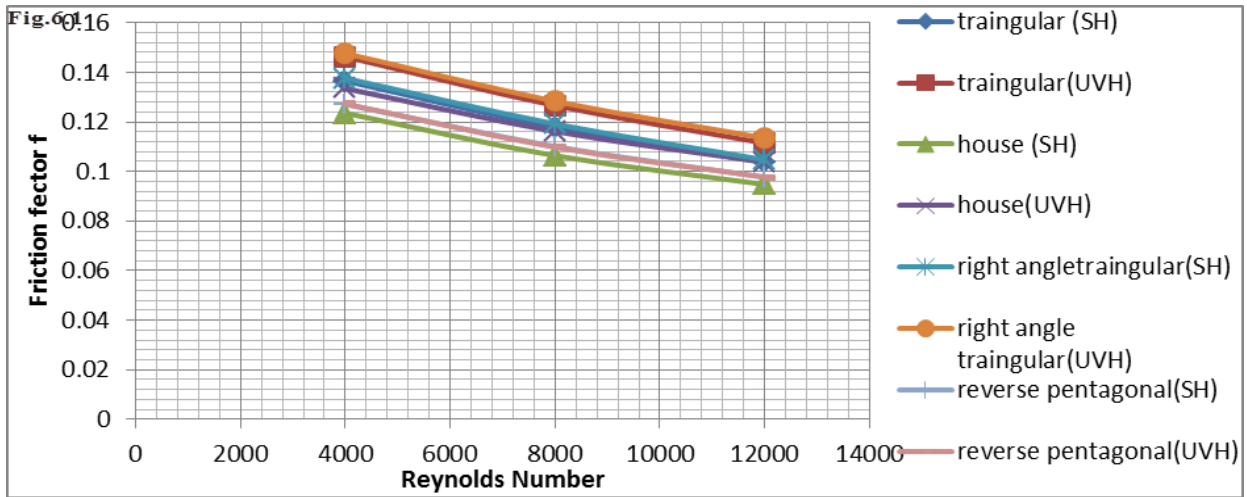


Fig. 19:

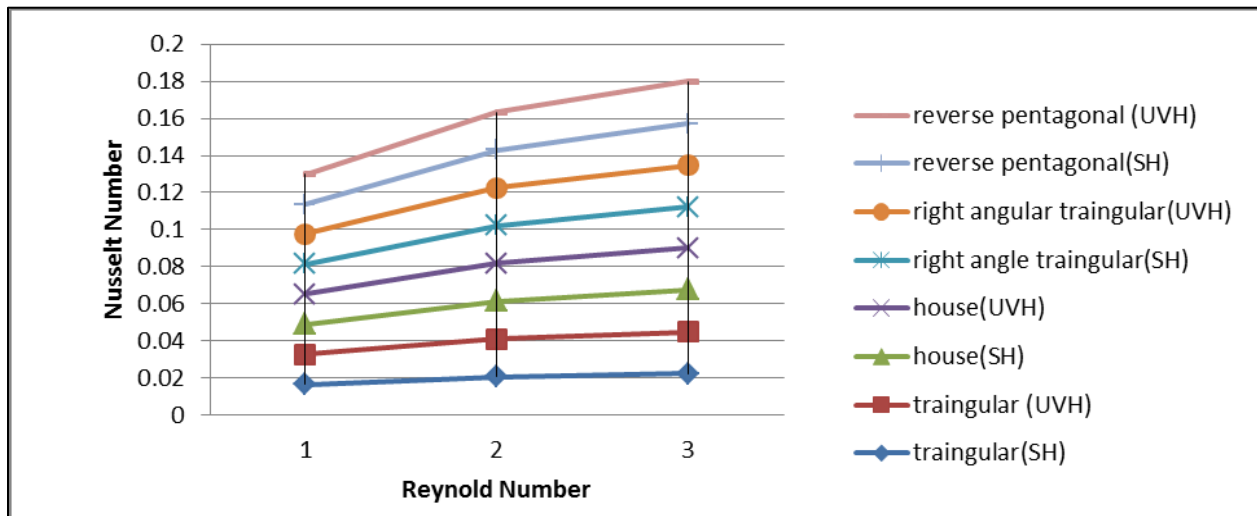


Fig. 20:

B. Effect of Rib Geometry:

The present CFD Analysis results on heat and flow friction characteristics in a uniform heat flux channel equipped with 1.598 mm rib height of eight different cross-sections: are presented in the form of Nusselt number and friction factor. The Nusselt numbers obtained under turbulent flow conditions for all rib-type tabulators with only one rib pitch ($P=22.91$ mm) are presented in Fig.2. In the figure, the rib tabulators yield considerable heat transfer enhancements with a similar trend in comparison with the smooth channel and the Nusselt number increases with the rise of Reynolds number. This is because the rib tabulators interrupt the development of the boundary layer of the fluid flow and increase the turbulence degree of flow. It is worth noting

that the triangular rib (SH) pointing downstream provides the highest value of Nusselt number while the reverse pentagonal rib (UVH) is found to perform better than the triangular rib (SH) pointing upstream. A close examination reveals that all the reverse pentagonal rib (UVH) and triangular rib (SH) yield higher heat transfer than the rectangular one for all Reynolds number values, similar to the result of Mi-Ae Moon, Min-Jung Park, Kwang-Yong Kim [1]. It is interesting to note that the in-line triangular rib (SH) provides almost the same values of Nusselt number as the reverse pentagonal (UVH) rib pointing downstream for all Reynolds numbers. For the inline reverse pentagonal (UVH) rib pointing downstream, the increase in Nusselt number value is about 20% over the smooth channel. The use of the triangular (SH) rib and reverse pentagonal (UVH) pointing downstream shows a higher heat transfer rate than that with the wedge (UVH) one at around 45%. The effect of using the rib tabulators on the isothermal pressure drop across the tested channel is presented in Fig. 6.2, The Decrease in friction factor for rib tabulators is considerably higher than that for the smooth channel and is also much higher than that in Nusselt number, however. This can be attributed to flow blockage, higher surface area and the act caused by the reverse flow.

C. Pressure Drop Results:

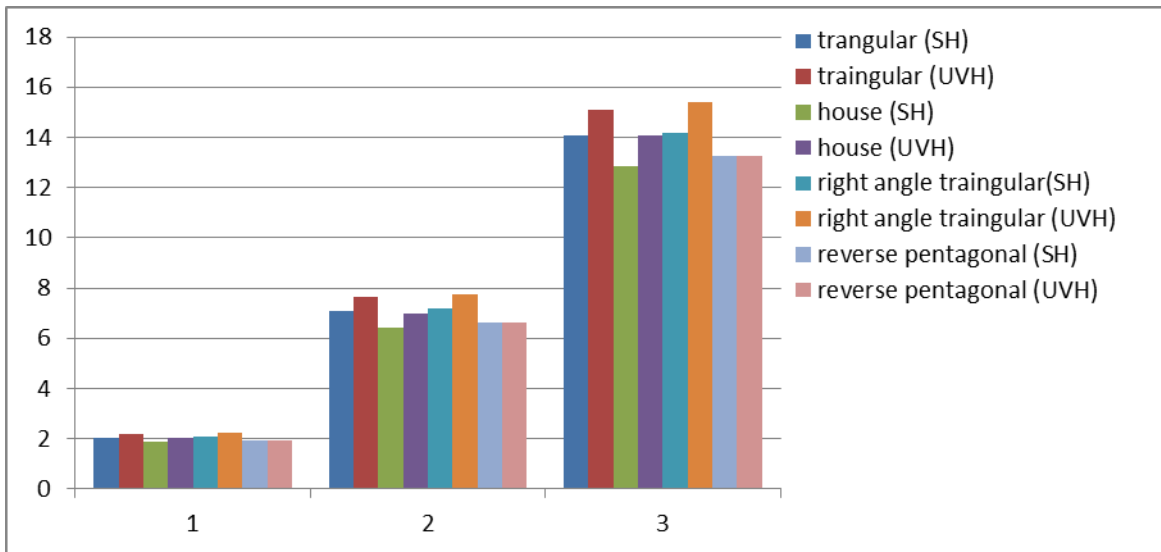


Fig. 21: Pressure drop in uniformly varying Height of various rib shapes

If the Reynolds number is defined based on hydraulic diameter, laminar flow is obtained for flow inside a round tube as long as the Reynolds number is less than about 2000, and this criterion appears to be a good approximate for smooth tubes regardless of the tube cross-sectional shape. Above this Reynolds number, the flow becomes unstable to small disturbances, and a transition to a turbulent type of flow generally occurs, although a fully established turbulent flow may not occur until the Reynolds number reaches about 12,000. However, in the present case of the ribbed and non-circular ducts, the flow is very complicated and the flow dynamics is not easily amenable to numerical solution. Therefore, the present CFD analysis data has been generated and are presented in this section. Early transition to turbulence and the turbulent flow-like behavior has been observed. It may be mentioned here that, in the present CFD analysis, the differential pressure drop has been measured at points far removed from the tube entrance where entry-length problem does not exist.

D. Heat Transfer Results:

Analytical and numerical heat transfer solutions have been obtained for rectangular smooth tubes simple channel geometries in much the similar manner. For both constant heat rate case and constant surface temperature case, the temperature is assumed to be constant around the tube periphery (which is not true for the present CFD analysis situation), and the conductance used in calculating Nu is an average with respect to peripheral area. An interesting feature of the solutions for shapes with sharp corners, like the square ducts, is the fact that the local heat transfer conductance varies around the periphery and approaches zero at corners; this means that the heat flux goes to zero at the corners.

A direct application of the analysis occurs in a plate-fin heat exchanger where the flow tubes are formed by thin fins extending between heated plates. A common assumption in the analysis of this arrangement is that the heat transfer coefficient is constant along the length of the duct. When the ribs are highly effective, i.e. when the ribs temperature is uniform and equal to the channel temperature, then the above analysis can be applied. But for the present CFD analysis situation, the heat transfer coefficient is not uniform along the ribs and the coil, and exact agreement of theoretical result and present CFD analysis data cannot be expected. Therefore, even if the simplified theoretical solutions are obtained, the simulation will not be exact replica of the real-life situation. In the present section, heat transfer results of the present investigation are discussed. In the present present

CFD analysis, the effect of duct geometry and ribs geometry on heat transfer characteristics is generally similar to that in case of pressure drop results, so only heat transfer results for combined rib(SH) and ribs(UVH) enhancement geometries are shown, Figs. 19–20. Heat transfer results for individual rib enhancement and coil enhancement geometry are not shown here. The present heat transfer results for only ribs compared well within $\pm 10\%$ and $\pm 8\%$ with Mi-Ae Moon, Min-Jung Park, Kwang-Yong Kim [1] correlation, Eq. (1) and S.W. Chang , T.-M. Liou , K.F. Chiang , G.F. Hong [2] correlation, Eq. (2), respectively. In the figures, $f Re$ and instead of f has been plotted along the ordinates since the product $f Re$ makes an easy comparison of the present data with the plain duct turbulent flow for which $f Re$ is constant ,whereas, in the present case, the product $f Re$ is not constant and it gives like a turbulent flow friction characteristics. In the heat transfer data plot, $Nu Y$ takes care of the viscosity correction due to fluid heating and the plain duct laminar flow Nusselt number under uniform wall heat flux boundary condition. $Re X$ takes care of the different values of the exponent of Pr in the different correlations for different cases (interpretations of X and Y are given in nomenclature).

VII. CONCLUSION

The heat transfer and friction loss performances of four cross-sectional rib shapes in a rectangular channel were evaluated. For the numerical analysis, three-dimensional RANS equations were solved using the Reynolds stress model with the SSG pressure–strain model. The computational results for the Nusselt number along the centerline of the heated surface were validated by comparison with experimental data for the channel with different ribs. The performance parameters related to the heat transfer and friction factor were found to strongly depend on the cross-sectional rib shapes. The reverse pentagonal (SH) shaped rib gave the best heat transfer performance with an average friction loss performance, and the right angle Triangular (UVH) rib gave the best friction loss performance. Except for the all rib, all the rib shapes with a vertical front wall showed the best heat transfer performances, while all the rib shapes with a vertical front surface showed the worst heat transfer performances with the largest recirculating zones behind the rib. Thus, the slope of the front surface of the rib, which affects the size of the recirculating zone, proved to be a critical factor to determining the heat transfer performance. However, the friction loss performance does not depend solely on the size of the recirculation zone between the ribs. Both the heat transfer and friction loss changed with the Reynolds number and pitch-to- rib width ratio, but the qualitative trends of the relative performances of the various rib shapes did not change with these two parameters. Both performances generally improved as the Reynolds number was increased. On the other hand, when the pitch-to-rib width ratio was decreased, the heat transfer improved while the friction loss became worse.

REFERENCES

- [1] J.C. Han, J.S. Park, M.Y. Ibrahim, Measurement of heat transfer and pressure drop in rectangular channels with turbulence promoters, NASA Contractor, Report 4015, 1986.
- [2] J. C. HAN, L. R. GLICKSMAN and W. M. ROHSENOW, AN INVESTIGATION OF HEAT TRANSFER AND FRICTION FOR RIB-ROUGHENED SURFACES Int. J. Heat Mass transfer(1978) Vol. 21, pp. 1143-1156
- [3] C.G. Spezial, S. Sarkar, T.B. Gatski, Modeling the pressure-strain correlation of turbulence: an invariant system dynamic approach, J. Fluid Mech. 227 (1991) 245–272.
- [4] M.E. Taslim, S.D. Spring, Effects of turbulator profile and spacing on heat transfer and friction in a channel, J. Thermophys. Heat Transfer 8 (1994) 555–562.
- [5] C.O. Olsson, B. Sundén, Heat transfer and pressure drop characteristics of ten radiator tubes, Int. J. Heat Mass Transfer 39 (1996) 3211–3220.
- [6] P.R. Chandra, M.L. Fontenot, J.C. Han, Effect of rib profiles on turbulent channel flow heat transfer, J. Thermophys. Heat Transfer 12 (1997) 116–118.
- [7] Akira Murata *, Sadanari Mochizuki, Effect of rib orientation and channel rotation on turbulent heat transfer in a two-pass square channel with sharp 180_ turns investigated by using large eddy simulation International Journal of Heat and Mass Transfer 47 (2004) 2599–2618
- [8] M. Amro a, B. Weiganda,*, R. Poser a, M. Schnieder An experimental investigation of the heat transfer in a ribbed triangular cooling channel. International Journal of Thermal Sciences 46 (2007) 491–500
- [9] S.W. Chang , T.-M. Liou, K.F. Chiang, G.F. Hong Heat transfer and pressure drop in rectangular channel with compound roughness of V-shaped ribs and deepened scales International Journal of Heat and Mass Transfer 51 (2008) 457–468
- [10] Pongjet Promvong, Chinaruk Thianpong Thermal performance assessment of turbulent channel flows over different shaped ribs International Communications in Heat and Mass Transfer 35 (2008) 1327–1334
- [11] Arvind Kumar, J.L. Bhagoria, R.M. Sarviya, Heat transfer and friction correlations for artificially roughened solar air heater duct with discrete W-shaped ribs. Energy Conversion and Management 50 (2009) 2106–2117
- [12] P. Liu, T. Gao, H. Mi, H. Liu, Numerical simulation of heat transfer and resistance pattern in channels with different ribs, Int. Conf. Comput. Des. Appl. 3 (2010) 507–511.
- [13] K. Wongcharee, W. Changcharoen, S. Eiamsa-ard, Numerical investigation of flow friction and heat transfer in a channel with various shaped ribs mounted on two opposite ribbed walls, Int. J. Chem. Reactor Eng. 9 (2011) (Article A26).
- [14] O. Manca, S. Nardini, D. Ricci, Numerical analysis of water forced convection in channels with differently shaped transverse ribs, J. Appl. Math. 211 (2011) (Article ID 323485, 25pp).
- [15] Giovanni Tanda, Effect of rib spacing on heat transfer and friction in a rectangular channel with 45_ angled rib turbulators on one/two walls International Journal of Heat and Mass Transfer 54 (2011) 1081–1090.
- [16] Mi-Ae Moon, Min-Jung Park, Kwang-Yong Kim, Evaluation of heat transfer performances of various rib shapes, International Journal of Heat and Mass Transfer 71 (2014) 275–284.